3D MSC/EMAS Simulation of a Three Phase Power Transformer by Means of Anisotropic Material Properties

Dr. E. Schmidt, S. Ojak

University of Technology Vienna
Institute for Electrical Machines and Drives
Gusshausstrasse 25-29
Vienna A-1040, Austria

Abstract

This paper deals with the MSC/EMAS simulation of a three phase power transformer using a 3D finite element model. The most important part of the presented simulation is the modelling of the multiturn windings and the iron core by means of anisotropic material properties. Characteristic calculation results with the derived transformer model will show that the modelling technique is practicable for many low frequency applications.

Introduction

In frequent cases both the high voltage and the low voltage windings of three phase power transformers consist of many single turns. Due to the high number of turns of the multiturn windings, it is impossible to model each turn with finite elements. Therefore, a replacement method of spreading the multiturn windings with a minimum of changes within the field and energy distribution is necessary.

The powerful technique of modelling multiturn windings using attached 0D circuit elements and 1D line elements [1,2] can be used in a wide range of multiturn windings. However, there are noticeable differences in the field and energy distribution in the regions of the windings due to the reduced number of turns of each winding. Because of this reason, it is necessary to develop another modelling method for multiturn windings when the fields of interest are the multiturn windings themselves.

The calculations are made using the finite element program MSC/EMAS in conjunction with the graphical user interface MSC/XL. Within MSC/EMAS each node in the finite element model has four degrees of freedom, the three components of the magnetic vector potential $\vec{\mathbf{A}}$ and the time integrated electric scalar potential ψ [5]. The field quantities are related to the potentials by

$$\vec{\mathbf{B}} = \operatorname{curl} \vec{\mathbf{A}} \ , \tag{1}$$

$$\vec{\mathbf{E}} = -\frac{\partial}{\partial t}\left(\vec{\mathbf{A}} + \operatorname{grad} \psi\right) \ . \tag{2}$$

The constitutive relations between the field quantities are used in the form

$$\vec{\mathbf{B}} = [\mu]\, \vec{\mathbf{H}} \ , \tag{3}$$

$$\vec{\mathbf{J}} = [\sigma]\, \vec{\mathbf{E}} \ , \tag{4}$$

$$\vec{\mathbf{D}} = [\epsilon]\, \vec{\mathbf{E}} \ , \tag{5}$$

where the three electromagnetic material properties (permeability μ, conductivity σ, permittivity ϵ) can be represented by anisotropic tensors in any cartesian, cylindrical or spherical coordinate system.

Throughout the calculations, fixed input voltages according to a three phase system are applied to the 3D finite element model. Therefore, the unsymmetric behaviour of three phase power transformers can be taken into account.

Transformer modelling

The new modelling method for multiturn windings is demonstrated on a simplified 3D model of a three leg power transformer with cylindrical windings as depicted in Figure(1). Figure(2) shows the detailed cross section of the transformer leg with the iron core, the high (HV) and low (LV) voltage coil windings and the surrounding air. In addition to the fundamental cartesian coordinate system a local cylindrical coordinate system is defined for each of the three transformer legs.

Figure 1: Please see next page

The dimensions of the iron core are chosen to maximize the iron core area within the circular cross section area of the windings [6]. First, the shown geometry is modelled for the three phases using 2D finite elements. Then the 3D finite element model is generated by successive extrude operations in the longitudinal direction of the transformer legs.

The material properties of the laminated iron core are built with anisotropic permeability and conductivity tensors related to the fundamental cartesian coordinate system,

$$[\mu]_{Fe} = \begin{bmatrix} \mu_{xx} & \mu_{xy} & \mu_{xz} \\ \mu_{yx} & \mu_{yy} & \mu_{yz} \\ \mu_{zx} & \mu_{zy} & \mu_{zz} \end{bmatrix} \quad , \quad [\sigma]_{Fe} = \begin{bmatrix} \sigma_{xx} & \sigma_{xy} & \sigma_{xz} \\ \sigma_{yx} & \sigma_{yy} & \sigma_{yz} \\ \sigma_{zx} & \sigma_{zy} & \sigma_{zz} \end{bmatrix} \quad . \tag{6}$$

The laminated iron core is represented by an effective permeability obtained from the ratio of airgap thickness to lamination thickness. At present, the different magnetization

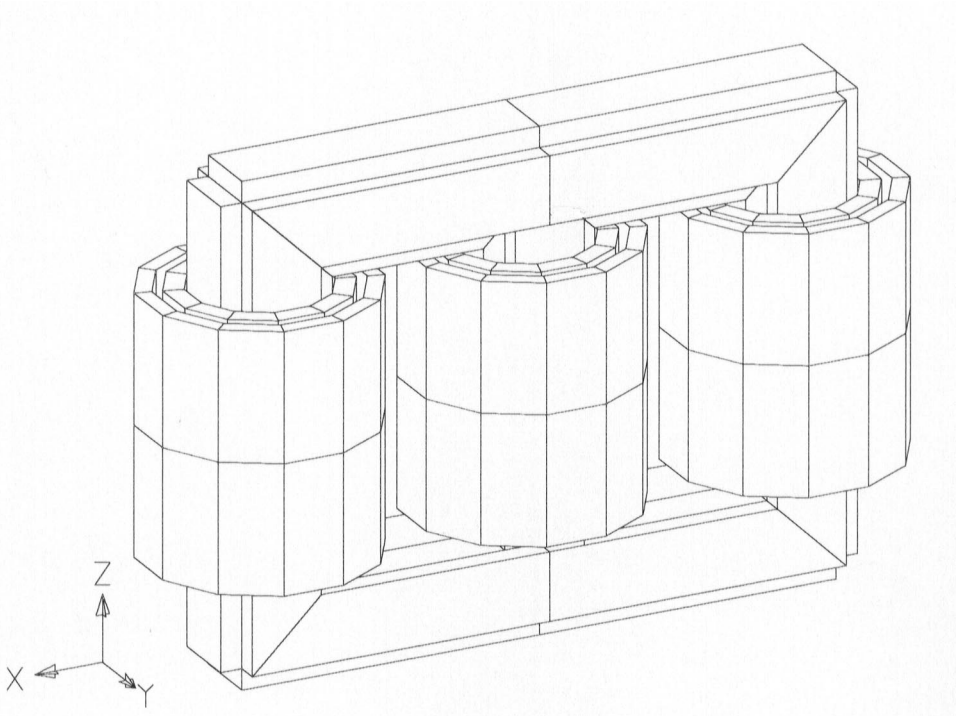

Figure 1: Three phase power transformer

directions (easy and hard) of the legs and yokes are not taken into consideration. Based upon the orientation of the cartesian coordinate system the anisotropic permeability and conductivity tensors can be written as

$$[\mu]_{Fe} = \begin{bmatrix} \mu_0\,\mu_r & 0 & 0 \\ 0 & \dfrac{\mu_0\,\mu_r}{(1-k_{Fe})\mu_r + k_{Fe}} & 0 \\ 0 & 0 & \mu_0\,\mu_r \end{bmatrix} \quad , \quad [\sigma]_{Fe} = \begin{bmatrix} \sigma_{Fe} & 0 & 0 \\ 0 & 0 & 0 \\ 0 & 0 & \sigma_{Fe} \end{bmatrix} \quad . \tag{7}$$

Figure 2: Please see the next page

The material properties of the high and low voltage coil windings are described with regard to the local cylindrical coordinate systems. Hence, the anisotropic conductivity tensor for each winding can be expressed as

$$[\sigma]_{Cu} = \begin{bmatrix} \sigma_{rr} & \sigma_{r\theta} & \sigma_{rz} \\ \sigma_{\theta r} & \sigma_{\theta\theta} & \sigma_{\theta z} \\ \sigma_{zr} & \sigma_{z\theta} & \sigma_{zz} \end{bmatrix} \quad . \tag{8}$$

Because of the applied voltage, there is no need to deal with an impressed current density in the coil windings. As there are no substantial eddy current effects in the multiturn windings, an assumption of the current density $\vec{\mathbf{J}}$ in the form of a spiral line with a constant ratio

$$c = \frac{J_z}{J_\theta} \tag{9}$$

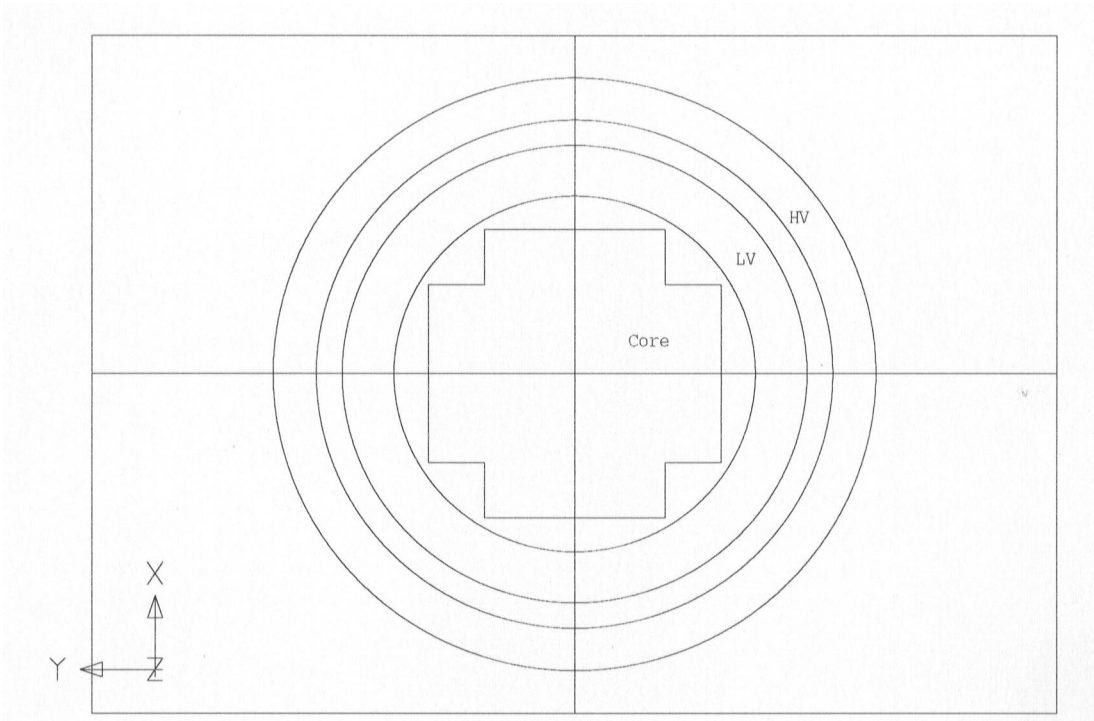

Figure 2: Cross section of the transformer leg

of the z component and the θ component of the current density is valid. Substituting this assumption into equation (4) yields for the anisotropic conductivity tensor of the multiturn coil winding

$$[\sigma]_{Cu} = \begin{bmatrix} 0 & 0 & 0 \\ 0 & \sigma_{Cu} & c\,\sigma_{Cu} \\ 0 & c\,\sigma_{Cu} & c^2\,\sigma_{Cu} \end{bmatrix} \quad . \tag{10}$$

The slope coefficients of the spiral lines can be derived easily from the geometry of the high voltage ($k = 1$) and low voltage ($k = 2$) coil windings [6]. From the height h_k, the average diameter d_k and the number n_k of turns per layer follows

$$c_k = \frac{h_k}{n_k d_k \pi} \quad , \quad k = 1,2 \quad . \tag{11}$$

Furthermore, the isotropic permeability μ_0 is assumed for the windings and the surrounding air, and for all materials the isotropic permittivity ϵ_0 is used.

To obtain a unique solution, the boundary conditions for the $\vec{\mathbf{A}}$ degrees of freedom are set in such a way as they keep the magnetic flux density tangential to the six outer planes of the whole model. In addition, the ψ degrees of freedom are constrained to zero on the lowest boundary of the iron core.

Transformer excitation and simulation results

The windings of the star-connected high voltage side are fed by a voltage source in form of a norton equivalent circuit derived from a current source excitation. The connection between the equivalent circuit and the high voltage windings is built using multipoint constraints for the ψ degrees of freedom as shown in Figure (3). Throughout the calculations, large capacitors are used for the external impedances connected to the high voltage windings. Therefore, the total magnetic energy and the total power losses of the transformer are obtained directly from the MSC/EMAS output [5].

Several detailed calculations representing any common operating condition are carried out to check the validity of the modelling method for the multiturn windings. The data reported here have been chosen to show some significant results for the star-connected low voltage side with a turns ratio $n_1/n_2 = 2$ and

- no-load condition,
- symmetric load condition with a $0.1\,\Omega$ resistor,
- short-circuit condition,

with applied voltages according to a symmetric three phase excitation.

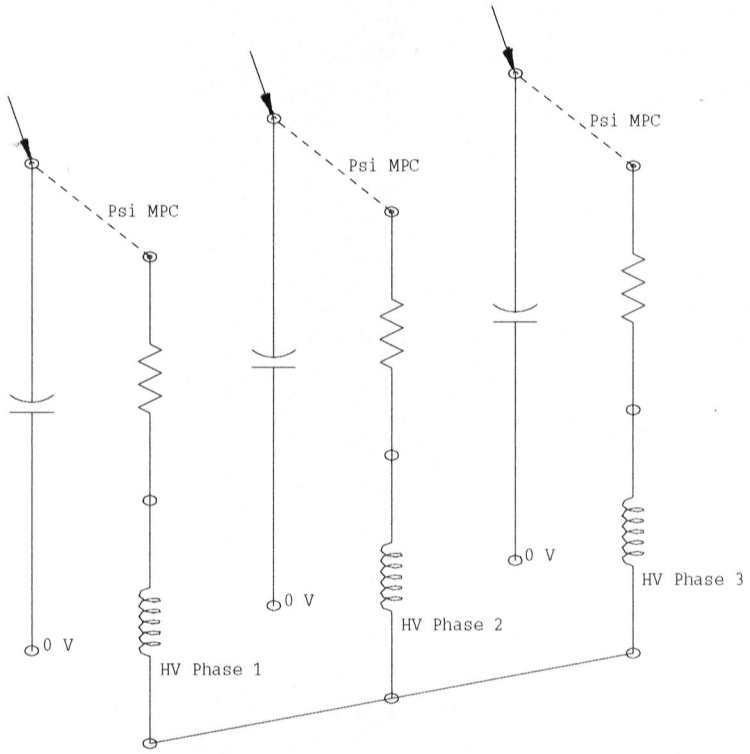

Figure 3: Equivalent circuit for the voltage source

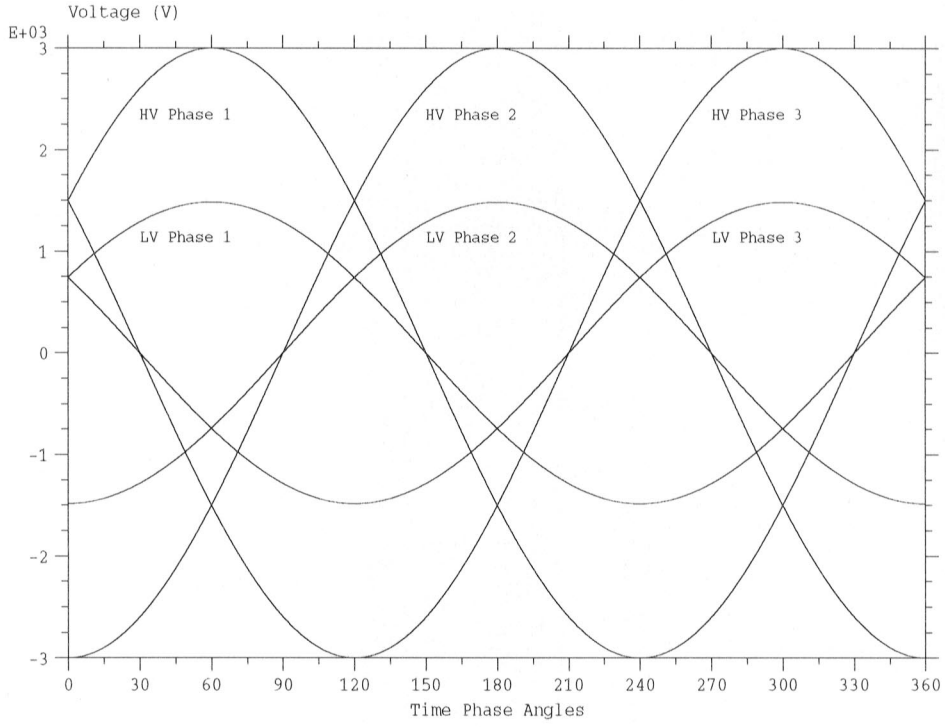

Figure 4: Phase voltages of the windings

Figure (4) shows the six phase voltages versus time phase angle for the no-load condition. The symmetry between the primary and the secondary voltages is in conformity with the turns ratio.

	Phase 1	Phase 2	Phase 3
Voltage	3 kV ∠300°	3 kV ∠180°	3 kV ∠60°
Current (grounded neutral)	80.4 A ∠210.2°	67.3 A ∠91.5°	82.8 A ∠330.2°
Current (nongrounded neutral)	77.8 A ∠210.1°	76.9 A ∠90.7°	78.0 A ∠330.9°

Table 1: Calculated phase currents under no-load condition

	Phase 1	Phase 2	Phase 3
Voltage	3 kV ∠300°	3 kV ∠180°	3 kV ∠60°
Current (grounded neutral)	8173 A ∠292.4°	8078 A ∠173.7°	8190 A ∠52.0°
Current (nongrounded neutral)	8168 A ∠293.3°	8151 A ∠173.4°	8184 A ∠53.3°

Table 2: Calculated phase currents under symmetric load condition

	Phase 1	Phase 2	Phase 3
Voltage	3 kV ∠300°	3 kV ∠180°	3 kV ∠60°
Current (grounded neutral)	67.34 kA ∠219.5°	67.09 kA ∠99.9°	67.42 kA ∠339.3°
Current (nongrounded neutral)	67.35 kA ∠219.7°	67.33 kA ∠99.7°	67.36 kA ∠339.7°

Table 3: Calculated phase currents under short-circuit condition

The computed phase current magnitudes under symmetric load condition correspond very well with those of the ideal transformer. Also the short-circuit condition values are in good agreement with the analytical short-circuit inductance [6,7]

$$L_s = \mu_0 \, n_1^2 \, \frac{d_s \pi}{h_s} \left(\frac{a_1}{3} + \delta + \frac{a_2}{3} \right) = 134 \mu H \quad . \tag{12}$$

The simulation results show some typical characteristics of the three phase transformer with three legs too. Because of the grounded neutral, the sum of the phase currents at the high voltage side is unequal zero. This is significant in comparison with the phase currents especially for the no-load condition.

	No-load	Symmetric load	Short-circuit
Grounded neutral	14.3 A ∠272.4°	251 A ∠300.6°	716 A ∠233.3°

Table 4: Sum of phase currents at the high voltage side with grounded neutral

The following table shows the necessary computer resources for the performed frequency domain calculations:

Number of Nodes	16700
Number of Elements	16560
Number of DOFs	59106
Computer used	DEC 3000-600 AXP
CPU used	21000 sec
IO used	30600 sec
Diskspace used	2200 MBytes

Conclusions

In this paper a new method for modelling multiturn windings is presented which gives good results in the cases where the leakage flux of the coil windings is of interest. The new modelling technique consists of using an anisotropic conductivity tensor for the coil windings, which is especially meaningful when applied voltages are used with the windings. The replacement method is used to analyse the behaviour of a three phase power transformer in case of typical load conditions with a 3D finite element model. The calculations with applied AC voltages demonstrate the usefulness of the model for simulations of unsymmetric winding faults in future research studies.

List of symbols

$\vec{\mathbf{A}}$	magnetic vector potential
$\vec{\mathbf{B}}$	magnetic flux density
$\vec{\mathbf{D}}$	electric displacement current density
$\vec{\mathbf{E}}$	electric field strength
$\vec{\mathbf{H}}$	magnetic field strength
$\vec{\mathbf{J}}$	electric conduction current density
L_s	short-circuit inductance per phase
a_1, a_2	radial thickness of the coil windings
c_1, c_2	slope coefficients of the spiral lines
d_1, d_2	average diameters of the coil windings
d_s	average diameter of the air-gap
h_1, h_2	heights of the coil windings

h_s	average coil height
k_{Fe}	filling coefficient of the laminated iron core
n_1, n_2	number of turns per layer of the coil windings
t	time
x, y, z	cartesian coordinates
r, θ, z	cylindrical coordinates
δ	air-gap between the coils
ϵ	permittivity
μ	permeability
σ	conductivity
ψ	time integrated electric scalar potential

References

[1] Brauer J.R., MacNeal B.E.: "Finite Element Modeling of Multiturn Windings with Attached Electric Circuits". *IEEE Transactions on Magnetics*, Vol.29, March 1993.

[2] Brauer J.R., MacNeal B.E., Hirtenfelder F.: "New Constraint Technique for 3D Finite Element Analysis of Multiturn Windings with Attached Electric Circuits". *IEEE Transactions on Magnetics*, Vol.29, November 1993.

[3] Jin J.M.: *The Finite Element Method in Electromagnetics*. John Wiley, 1993.

[4] Miri A.M., Hauser A.O., Rwakasenyi S.: "3D Calculation of Transient Potential Distribution in High-Voltage Transformer Windings". Proceedings of the 20th MSC European Users Conference, Vienna, 1993.

[5] *MSC/EMAS Users Manual, Version 3.* The MacNeal-Schwendler Corporation, Los Angeles, 1994.

[6] Ojak S.: "Erstellung eines dreidimensionalen Finite-Elemente-Modells für einen Drehstrom-Transformator". Diploma thesis, TU Wien, 1995.

[7] Richter R.: *Elektrische Maschinen, Band 3, Transformatoren.* Birkhäuser, 1963.